RSC Advances

ROYAL SOCIETY OF CHEMISTRY

www.rsc.org/advances

Journal Name

RSCPublishing

ARTICLE

In vivo evaluation of an anticancer drug delivery system based on heparinized mesoporous silica nanoparticles

Cite this: DOI: 10.1039/x0xx00000x

Received 00th January 2012,
Accepted 00th January 2012

DOI: 10.1039/x0xx00000x

www.rsc.org/

Qiang Wu,*[a] Ruifang Li,*[b] Chao Zhao,[a] Jiejie Ren,[a] Keyuan Du,[a] Baoqing Yin,[a] Junmin Fu,[b] Xiangjun Qiu[b] and Chunsheng Gao[c]

In this study, a heparinized mesoporous silica nanoparticles (denoted as MSNs-HP) was used for loading anticancer drug. MSNs-HP was found capable of penetrating into cancer cells and delaying the release of anticancer drug doxorubicin (DOX) according to its in vitro and in vivo release profiles. Much interesting, in vivo evaluation on the animal xenograft models showed that the tumor inhibitory rate of loaded MSNs-HP (58%) was much more than that of DOX inside nanoparticles alone (18%) and close to that large doses of DOX (67%, 7-fold higher in dosage than DOX inside nanoparticles), indicating that the use of MSNs-HP was able to significantly increase the antitumor efficacy of DOX. As to the reason of this nanoparticles-drug system against tumor growth, the synergy of these two components in inducing tumor cell apoptosis and tumor necrosis and inhibiting tumor angiogenesis might be responsible for. Furthermore, this system was found safer than large doses of drug. All the above might enable MSNs-HP to be a potentially high-efficiency and low toxicity carrier for anticancer drug delivery.

Introduction

Heparin, a highly sulfated glycol-saminoglycan, is a well-known anticoagulant. Except for the anticoagulant activity, heparin has also shown other activities, such as the regulation for the complement activity and inflammation, the participation in the release of lipoprotein lipases, the control of tumor growth by inhibiting tumor angiogenesis and metastasis and et al.[1-6] The diverse activities give heparin the potential to be exploited for therapeutic use to treat many different ailments and diseases. Recently, research has begun to combine the useful biological activities of heparin with the useful properties of nanomaterials. The combination of these two substances can provide synergistic improvements enhancing already existing properties, and also create novel applications ranging from improving anticoagulant activity for anticancer therapy to tissue engineering and biosensors.[1] In particular, heparin is of interest for use as a drug delivery system (DDS) in the treatment of cancers. Up to now, various heparin-based DDSs have been developed, in which the role of heparin is not only to improve blood compatibility of nanomaterials but also to serve as an effective drug for cancer therapy.[7-11]

Mesoporous silica nanoparticles (MSNs) is a class of very promising candidate for anticancer drug delivery due to its biocompatibility and preferential accumulation in tumors.[12-14] To further improve the performances of MSNs in cancer therapy, its surface is often functionalized with various bioactive molecules. For example, the modification of polyethylene glycol (PEG) derivatives is able to improve the dispersion of nanoparticles in saline, increase their circulatory half-life, reduce their uptake by reticular-endothelial system (RES) and thus enhance the enhanced permeability and retention (EPR) effect.[15,16] The conjugation of specific ligands, such as folic acid and mannose, allows the targeting of nanoparticles to cancer cells.[14,17] Although these MSNs-based DDSs along with their functional molecule are well-established or well-defined via in vitro assays, the in vivo evaluations always exhibit unexpected results due to the complicated physiological environment. For example, camptothecin-loaded folic acid-MSNs conjugates showed a higher cell killing in the in vitro study and a greater accumulation in tumors than unloaded conjugates, but no significant difference was found in the tumor-suppressing effect when these two systems were transferred into animal xenograft models.[14] This result may be correlated with high dosage of drug injections that could suppress the tumors very quickly and then mask the enhanced effect of carriers, and low expression of folate receptor on tumor cells. Therefore, the most critical question regarding the

use of functionalized MSNs in cancer therapy is its actual efficacy for suppressing tumors growth. In our previous study, a type of heparinized magnetic MSNs with good dispersity and blood compatibility has been developed for growth factor delivery.[18] Herein, heparin was again covalently bound to the surfaces of bare MSNs. The resultant composite was denoted as MSNs-HP and used for loading anticancer doxorubicin (DOX). Then, drug release profile from the composite and uptake of the composite itself by cancer cells were investigated. Finally, antitumor effect and safeness of DOX-loaded composite were evaluated on tumor-bearing mice models. The aim is to develop an effective carrier for anticancer drug delivery.

Materials and methods

Materials

Tetraethyl orthosilicate (TEOS), cetyltrimethlammonium bromide (CTAB), 3-aminopropyltriethoxysilane (APTES), polyvinyl pyrrolidone (PVP30, MW 30,000), heparin sodium (MW 12,000) and DOX were purchased from Shanghai Chemical Corp. N-hydroxysuccinimide (NHS), 1-ethyl-3-(3-dimethylaminopropyl) carbodiimide-hydrochloride (EDC), 4-morpholineethanesulfonic acid (MES), 1,1'-dioctadecyl-3,3, 3',3'-tetramethylindocarbocyanine perchlorate (DiI), fluorescein isothiocyanate (FITC), (2'-(4-ethoxyphenyl)-5-(4-methyl-1-piperazinyl)2,5'-bi-1H-benzimidazoletri hydro chloride) (Hoechst 33342), and toluidine blue were obtained from Sigma-Aldrich (USA). Basic fibroblast growth factor (bFGF) was purchased from Pharmacia (Sweden). The antibodies used for western-blot were purchased from Santa Cruz Biotechnology (USA). All other chemicals are of analytical grade.

Synthesis of FITC-APTES

A solution of FITC (8.6 mg) in anhydrous ethanol (2 mL) was mixed with APTES (0.197 mL) and then the mixture was stirred at room temperature for 24 h. The prepared FITC-APTES stock solution was kept at 4 °C.

Synthesis of amino-modified MSNs (denoted as MSNs-NH_2)

The synthesis of MSNs-NH_2 was similar to that of magnetic MSNs-NH_2.[18] Typically, 0.3 g CTAB and 0.1 g PVP30 were added to a solution contains 90 mL of deionized water and 60 mL of methanol. The solution was adjusted to pH 10.2 by ammonia solution, and then 600 μL of TEOS and 50 μL of APTES were added. After stirring for 2.5 h at room temperature, the resultant particles were separated and washed with ethanol and water. The extraction of organic templates for the as-synthesized particles was performed by dispersing these particles into 50 mL of the mixed solution of ethanol and NH_4NO_3 (0.3 g) at 60 °C for 1 h. The synthesis of FITC-labeled MSNs-NH_2 is similar to that of unlabeled one, except FITC-APTES (50 μL) and APTES were added in together during condensation process.

Synthesis of MSNs-HP and FITC-labeled MSNs-HP

The immobilization of heparin onto MSNs-NH_2 and FITC-labeled MSNs-NH_2 was performed according to our previous report.[18] Typically, 100 mg of MSNs-NH_2 or FITC-labeled MSNs-NH_2 were suspended in 30 mL of 0.1 M MES buffer (pH 5.5) and hydrated for 2 h, to which EDC (287.4 mg) and NHS (172.8 mg) were added, and then 20 mg of heparin was slowly added. The reaction mixture was incubated at 4 °C by rotating overnight. Samples were collected by centrifugation and then dialyzed against deionized water to get rid of the residual EDC, NHS and heparin. The obtained products were lyophilized and kept at 4 °C. The content of heparin incorporated into MSNs-NH_2 was examined by toluidine blue assay.[19]

The loading/release of DOX into/from MSNs-HP

MSNs-HP (100 mg) was dispersed in 20 mL of DOX solution (0.5 mg mL^{-1}). After shaking for 24 h under dark condition, the solid particles were centrifuged and washed with PBS solution (pH 7.4). To evaluate the loading efficiency of drug, the supernatant solutions were collected and the residual drug was measure by UV-vis spectroscopy at 480 nm. The loading efficiency of drug was expressed as percentage of drug in MSN-HP with respect to the initial amount of drug.

The in vitro release test was performed by immersing the drug-loaded sample (10 mg) in 10 mL of PBS solution. The suspension was gently shaken at 37 °C in a water bath. At given time, the medium was replaced with fresh medium. The amount of the released DOX from MSNs-HP was determined by UV-vis spectrophotometer. To determine the amount of DOX left in the nanoparticles at the end of the release test, the nanoparticles were collected and dissolved by 2 M NaOH. Then, the undissolved DOX was separated and again dissolved by 1 M HCl. Finally, the remained drug was quantified by UV-vis spectrophotometer.

The concentration profile of DOX in rat plasma

MSNs-HP containing 4% of DOX was intravenously administered via a sublingual vein of a male Sprague–Dawley rat (200 ± 20 g) as a single dose of 8 mg kg^{-1} (in which the content of DOX was 0.32 mg). Blood was sampled from the tail vain at each time interval, and blood samples (1 mL) were collected by heparinized tubes, and then centrifuged at 2500 g for 15 min at 4 °C to separate the plasma and stored at − 20 °C until analysis. Subsequently, the plasma (300 μL) was mixed with 20 μL of daunorubicin internal standard (20 μg mL^{-1}) and 50 μL of hydrochloric acid solution (1 mol L^{-1}), and then the suspension was extracted with 1 mL of ethyl acetate for 2 min. After standing stratification, the upper organic layer was transferred to another tube and evaporated to dryness at 40 °C under a stream of nitrogen (about 40 min). The residue was dissolved in 100 μL of the HPLC mobile phase (65% of H_2O, 25% of acetonitrile and 10% of trifluoroacetic acid) by vortexing and 20 μL of solution was used for the measurement of DOX concentration with a HPLC system (HP Agilent 1100). The flow rate of the mobile phase was 0.8 mL min^{-1}. Detection wavelength was 210 nm.

Cell culture

Hela cells, HepG2 cells and H22 mouse sarcoma cells were originally obtained from Shanghai Institute of Biochemistry and Cell Biology (Chinese Academy of Sciences). The cells were maintained in Dulbecco's modified Eagle's medium (DMEM, GIBCO) supplemented with 10% fetal calf serum, 2% L-glutamine, 1% penicillin, and 1% streptomycin stock solutions, and then seeded in a 96-well plate at a density of 10^4 cells per well and cultured in 5% CO_2 at 37 °C for 24 h.

The uptake of FITC-labeled MSNs-HP by Hela cells

The cellular uptake of FITC-labeled MSNs-HP was investigated by high content screening (Thermo Scientific ArrayScan VTI 600). In brief, 1.0×10^5 of Hela cells were incubated with nanoparticles in an 8-well plate for 30 min and then washed with DMEM and PBS to remove nanoparticles that did not enter the cells. The cells were then stained with Hoechst 33342 and DiI before measurement.

Establishment of the H22 xenograft model

50 Male Kunming mice (8-10 weeks old, Code number SCXK2010-0007) weighting 18-22 g were obtained from the Medical Experimental Animal Center, Henan Province, China. The H22 model was established by subcutaneous injection as previously described,[20] in which 0.2 mL of H22 cell suspensions (1.0×10^6 cells/mL) were subcutaneously inoculated into the right armpit region of mice. The experimental procedures described in this section and the previous section to investigate the concentration profile of DOX in plasma by using of male Sprague–Dawley rat were performed in accordance with the Guidelines of Animal Experiments from the Committee of Medical Ethics, National Health Department of China (1998) and followed standards and policies of the Henan University of Science and Technology's Animal Care and Use Committee.

Animal groups and treatments

Twenty-four hours after establishment of the H22 models, the transplanted mice were allocated to five groups (10 mice in each group) as follows treatment: normal saline (control group), MSNs-HP nanoparticles (8 mg kg^{-1}), DOX-loaded MSNs-HP nanoparticles (8 mg kg^{-1}), low doses of DOX (0.3 mg kg^{-1}) and high doses of DOX (2.0 mg kg^{-1}). These agents were denoted as control, unloaded MSNs-HP, loaded MSNs-HP, DOX0.3 and DOX2.0 respectively. All the agents were injected 1 time/per day via the lateral tail vein and body weight was daily checked. After 10 days, the antitumor activity was evaluated by weighing the tumor tissues. The tumor inhibitory rate (%) was calculated as: (1-(average tumor weight of each group)/(average tumor weight of control group)) × 100%. Herein, it should be noted that the amount of loaded MSNs-HP administrated was approximately equal to the sum of unloaded MSNs-HP and DOX0.3.

Histomorphometric determination

The tumor tissue was fixed in 10% formalin, and then dehydrated, embedded in paraffin blocks, cut into 5 μm sections, and finally mounted on APTES-coated slices. In the next, sections were deparaffinized, rehydrated, washed with H_2O, stained with hematoxylin-eosin (HE) and finally observed under a light microscope at 100 × and 400 × magnification.

Western blot analysis

Tumor tissues were homogenized in lysis buffer containing proteinase inhibitors and then western blotting was performed as previously described.[21,22] Briefly, equal amounts of protein (60 μg) quantified by Bradford method were separated by 12% SDS-PAGE and then transferred onto PVDF membranes at 100 V for 60 min. Blocking solution (5% skim milk) was loaded over membranes for 1 h at room temperature. The membranes were incubated with Bcl-2, Bax, VEGF polyclonal antibody and β-actin antibody (1:1,000 dilution) respectively overnight at 4 °C, then incubated with responding horseradish peroxidase-labeled secondary antibodies at room temperature for 1 h. Finally, immuno-reactivity was detected by the enhanced chemiluminescence method. Quantization of protein band density was performed using Gel-Pro Analyzer 4.0. Data are reported as normalized protein band density.

Blood biochemistry and immune function analysis

At the end of tumor growth assays, blood was collected from the eye-orbit of the transplanted mice and left at room temperature for 30 min. Then, the blood samples were centrifuged at 4 °C for 10 min. The separated serum was stored at -70 °C for biochemical analysis. Finally, biochemical criterions such as aspartate aminotransferase (AST), alanine aminotransferase (ALT), blood urea nitrogen (BUN), creatinine, white blood cell count, thymus index and spleen index were measured.

MTT assays

To study the interaction between DOX and MSNs-HP, HepG2 cells were treated with various dilutions of DOX in the presence or absence of MSNs-HP, cell viability was determined after 48 h and IC_{50} values were determined by plotting the percentage of cell survival as a function of DOX or MSNs-HP concentration. The interactions between DOX and MSNs-HP were evaluated by the combination index (CI) (synergism, additive effect, and antagonism) according to Chou and Talalay equation.[23] For 50 percent toxicity, the combination index (CI) values were calculated based on the equation stated below: Combination Index (CI) = (D)1/(Dx)1 + (D)2/(Dx)2. where (Dx)1 is dose of DOX to produce 50 percent cell kill alone; (D)1 is dose of DOX to produce 50 percent cell kill in combination with MSNs-HP; (Dx)2 is dose of MSNs-HP to produce 50 percent cell kill alone; (D)2 is dose of MSNs-HP to produce 50 percent cell kill in combination with DOX.

Chicken chorioallantoic membrane assay (CAM)

To investigate the effect of MSNs-HP on growth factor-induced angiogenesis, the CAM assays in vitro were performed

according to the previous report.[24] Briefly, the embryos were allocated to four groups (8 eggs in each group) as follows treatment: normal saline (control), bFGF (100 ng), bFGF (100 ng) + heparin (10 μg) and bFGF (100 ng) + MSNs-HP (100 μg). After incubation at 37 °C for 10 days in a humidified atmosphere, fertilized eggs were opened and the shell membranes were taken off in order to expose chorioallantoic membranes. Then, the above agents in PBS were applied to the top of chorioallantoic membrane and the windows were recovered with glass-adhesive plaster and the fertilized eggs were incubated continuously for another 96 h. Finally, the chorioallantoic membranes were taken off and fixed with formaldehyde. The tube formation of CAM was monitored by BI-2000 photograph system.

Statistical analysis

Data were expressed as mean ± S. D. Statistical analysis was performed by Student's *t* test and one-way analysis of variance (ANOVA) followed by Dunnett's post hoc test when appropriate. Differences were considered statistically significant at $P < 0.05$.

Characterization

Transmission electron microscopy (TEM) analyses were conducted on a JEM-2100F electron microscope operating at 200 kV. UV-Vis spectra were recorded on UV-3101PC Shimadzu UV-vis spectroscope. Nitrogen adsorption-desorption isotherms at 77 K were measured on a Micrometitics Tristar 3000 system. Zeta potentials of nanoparticles were measured by Malvern Zetasizer Nano ZS90. Fluorescence images were obtained by Leica DMI4000B fluorescence microscropy.

Results and discussion

The characterization of MSNs-HP and its drug-releasing behavior

The preparations of MSNs-HP and its drug-loaded sample were performed partially according to our previous report[18] and the details were described as follows: (i) synthesis of MSNs-NH_2 using sol–gel methods incorporated by APTES, (ii) conjugation of heparin with MSNs-NH_2 via carbodiimide chemistry, and (iii) loading of DOX into heparinized MSNs by physical adsorption. As shown from SEM and TEM images (Fig. 1a and 1b), MSNs- NH_2 substrate exhibits a very uniform particle size distribution around 120~160 nm, a regular spherical morphology, a disordered porous structure, and a perfect mono-dispersivity. The immobilization of heparin onto MSNs-NH_2 has no effect on its morphology (data not shown), but the BET surface area, pore volume, pore size and the zeta potential of MSNs-NH_2 reduced from 552 $cm^2\ g^{-1}$, 0.74 $cm^3\ g^{-1}$, 2.58 nm and 34 mV to 329 $cm^2\ g^{-1}$, 0.40 $cm^3\ g^{-1}$, 2.07 nm, and –43 mV respectively (Fig. 2a and 2b and Fig. S1a and S1b), and the immobilization efficiency was approximately 2% (w/w) as determined by toluidine blue assay. Furthermore, 4% (w/w) of DOX loading capacity onto MSNs-HP was confirmed by UV–vis measurements at the wave-length of 480 nm. The in vitro release profile of DOX from nanoparticles was shown in Fig. 3a. It can be seen that the burst release of drug occurred within the initial 8 h. After 70 h, the release curve reached a plateau and only around 70% of the drug was released out. The further drug release was not found at the end of the study. According to the dissolution experiment of material (please see the experimental section), the other 30% of drug was still inside the nanoparticles. When loaded MSNs-HP was intravenously administered, it can be seen from Fig. 3b that the peak concentration state of DOX inside nanoparticles in plasma could be maintained up to 6 h, its whole concentration profile of a single dose of administration was sustained up to 72 h, and the calculated half-life was approximately 20.5 h, whereas the concentration profile of DOX administration alone was reported to be lower than 10 min.[7] These results suggested that MSNs-HP was able to extend circulation of drug and thus could be helpful for improving therapeutic efficacy. Herein, the high dosage of drug incorporation into the materials and the controlled drug release might be attributed to porous and electrostatic interaction between negatively charged heparin and positively charged DOX.

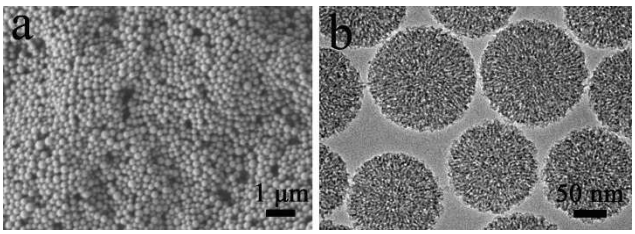

Fig. 1 SEM (a) and TEM (b) images of MSNs-NH_2.

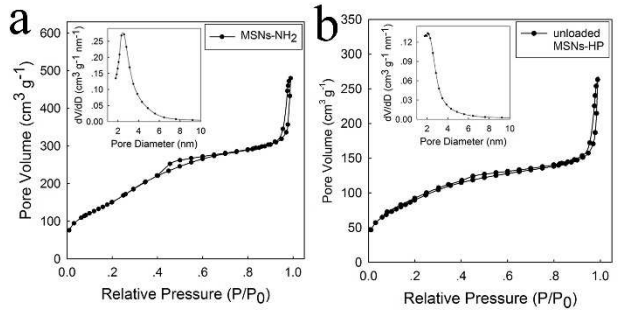

Fig. 2 Nitrogen adsorption-desorption of MSNs-NH_2 (a) and MSNs-HP (b). The inset was the corresponding pore size of these nanoparticles.

Cellular uptake analysis

Cellular uptake is considered as a prerequisite for those nanoparticles to be developed as drug delivery carriers administrated by intravenous injection. Then, we labeled MSNs-HP with FITC dye and investigated its interaction with Hela cells using High Content Screening. As shown in Fig. 4a, FITC-labeled MSNs-HP alone exhibited strong green fluorescence emission. Fig. 4b showed the fluorescence images of Hela cells in the presence of Hoechst 33342 and DiI dye. It can be seen that cell nuclei stained with Hoechst 33342

exhibited blue fluorescence; cell membranes stained with DiI exhibited red fluorescence; cytoplasm also exhibited red fluorescence due to the diffusion of DiI from cell membranes to cytoplasm. Fig. 4c showed the merged image of Hela cells in the presence of FITC-labeled MSNs-HP and the other two dyes. It can be seen that cell nuclei still exhibited blue fluorescence, but the fluorescence of cell membranes and cytoplasm changed from red to yellow green due to the overlapping of red fluorescent spots and green fluorescent spots, indicating that MSNs-HP could penetrate into the living cells. Herein, it should be mentioned that MSNs-HP is negative charged which is not benefit its cellular uptake. The great cellular uptake of nanoparticles may be related to the heparin target effect because lots of natural products such as bleomycin also have tumor targeting properties.[25]

Tumor suppression analysis

Having verified the uptake of MSNs-HP by cancer cells, solid H22 tumors were then established in mice to determine whether DOX-loaded MSNs-HP can suppress tumor growth in vivo. As shown in Fig. 5, the administrations of unloaded/loaded MSNs-HP, DOX0.3 and DOX2.0 all exhibited the inhibition on the tumor growth relative to the saline control. Interestingly, although the DOX dosage in loaded MSNs-HP was approximately 7-fold lower than that of DOX2.0, its inhibitory efficiency (58%) was only a little lower than that of the later (67%) and much more than those of DOX0.3 (18%, in which the DOX dosage was equal to that of loaded nanoparticles) and unloaded MSNs-HP (20%, see Table 1). Bcl-2 is a protein that can protect cells from external insults and afford anti-apoptotic properties. Bax is a protein that can oppose the anti-apoptotic activity of Bcl-2. The Bcl-2/Bax ratio as an apoptosis index is believed to determine whether tumor cells undergo apoptosis.[26] Fig. 6 showed the expression of Bcl-2 and Bax protein in the tumor tissues of mice treated with different agents. It can be seen that all the agents except the saline control caused the decrease of Bcl-2/Bax ratio, indicating their apoptosis-inducing activities. Likely, the similar tendencies as those observed in tumor growth assays also appeared, in which the ratio induced by loaded MSNs-HP was close to that induced by DOX2.0 and less than those induced by unloaded MSNs-HP and DOX0.3. Furthermore, histological examination of solid tumors showed the presence of a large size areas of tumor necrosis in the loaded MSNs-HP-treated and DOX2.0-treated mice, whereas tumor necrosis induced by unloaded MSNs-HP and DOX0.3 was clearly lower than those induced by the above two agents (Fig. 7). The similar performances of loaded MSNs-HP in above investigations as those of DOX2.0 rather than those of DOX0.3, as well as the positive performances of MSNs-HP itself suggested that MSNs-HP play a synergistic role in antitumor with DOX and greatly improved its efficacy. The synergy of MSNs-HP and DOX was further verified by cell viability assays, in which the combination index (CI) of these two components against the proliferation of HepG2 cells was clearly less than 1 at medium dose levels (IC_{50}) for MSNs-HP/DOX (Table. S1 and Fig. S2). All of these make the resultant DDS system highly effective in suppressing tumor growth.

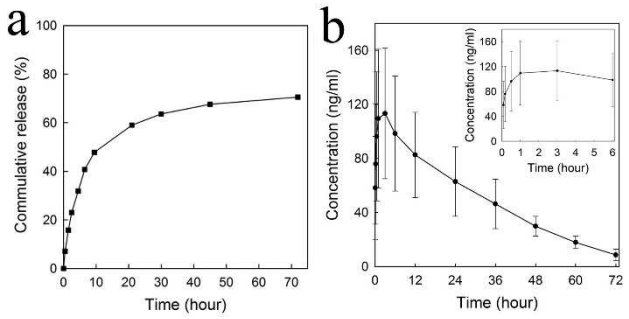

Fig. 3 (a) Release profile of DOX from MSNs-HP in PBS solution (pH7.4). (b) Plasma concentration–time curve of DOX following the administration (i.v.) of a single dose of loaded MSNs-HP (8 mg kg^{-1}) in normal Sprague–Dawley rat. The inset was the profile of the initial peak concentration of drug in plasma.

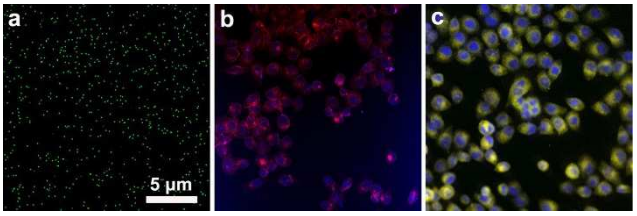

Fig. 4 Fluorescence image of FITC-labeled MSNs-HP (a); High content screening image of Hela cells stained with Hoechst 33342 (blue fluorescence) and DiI (red fluorescence) simultaneously (b); High content screening image of Hela cells in the presence of Hoechst 33342, DiI and FITC-labeled MSNs-HP (c).

Tumor angiogenesis analysis

Growth factors such as vascular endothelial growth factor (VEGF) and bFGF play a crucial role in angiogenesis,[27] a key event during tumor formation. DOX and heparin were reported to be able to inhibit angiogenesis by decreasing the expression

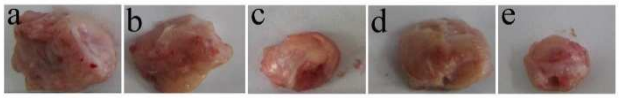

Fig. 5 The effects of different agents on the tumors growth in transplanted H22 mice: control (a); unloaded MSNs-HP (b); loaded MSNs-HP (c); DOX0.3 (d); DOX2.0 (e).

Table 1 The effects of different agents on the tumor growth in transplanted H22 mice. (mean ± S. D., n = 10)

Groups	Weight (g)		Tumor weight (g)	Inhibitory rate (%)
	Pre-treatment	Post-treatment		
Control	19.5 ± 2.5	24.7 ± 2.9	1.6 ± 0.2	—
unloaded MSNs-HP	20.7 ± 2.0	27.2 ± 3.5	1.3 ± 0.2*	20.5#
Loaded MSNs-HP	23.0 ± 2.4	28.9 ± 3.1	0.7 ± 0.3*#	58.8
DOX0.3	22.3 ± 1.2	29.3 ± 2.5	1.3 ± 0.3*#	18.0#
DOX2.0	21.2 ± 3.6	22.6 ± 5.1	0.5 ± 0.2*#	67.5

* $P < 0.05$, compared to control group; # $P < 0.05$, compared to DOX2.0 group.

of these pro-angiogenetic factors in tumor tissue or disrupting their interaction with endothelial cell-surface receptors.[6,28] Fig. 8 showed the expression of VEGF in xenograft tumors treated with different agents. It can be seen that all the agents except the saline control were able to decrease protein expression and loaded MSNs-HP exerted the strongest inhibitory effect. Furthermore, it has been reported that several heparinized nanomaterials were capable of disturbing growth factors-induced angiogenesis.[29-31] We then examined the effect of MSNs-HP itself on the pro-angiogenetic activity of growth factors by the CAM assays in vitro. Fig. 9 showed the

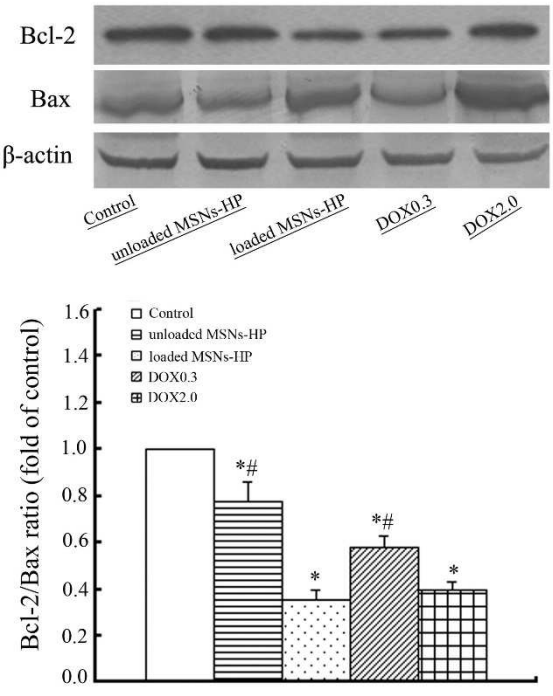

Fig. 6 The expression of Bcl-2 and Bax protein in the tumor tissue of transplanted H22 mice treated with different agents (up) and the analysis for the Bcl-2/Bax ratio (down). (* $P < 0.05$ *vs* control group and # $P < 0.05$ *vs* unloaded MSNs-HP group).

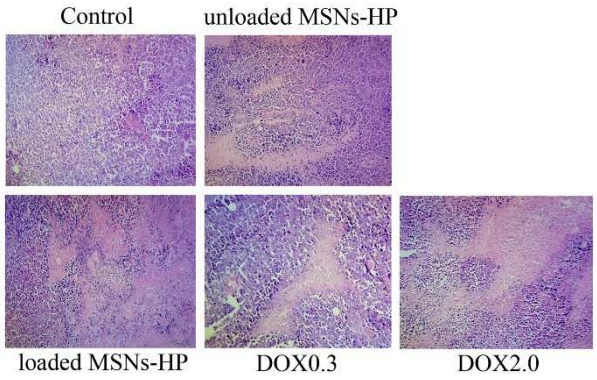

Fig. 7 Histological examination of solid tumors in H22 transplanted mice treated with different agents (100 × magnification). Cell nuclei were stained with blue and necrosis areas without cell nuclei were shown with light red.

formation of new blood vessels of the CAM models in the presence of different agents. It can be seen that growth factor bFGF induced a pronounced angiogenetic response in the treated model compared to the control (Fig. 9a and 9b), whereas the presence of heparin or MSNs-HP seriously disturbed such a response (Fig. 9c and 9d). Therefore, loaded MSNs-HP could have multiply of antitumor actions, by first inducing tumor cell apoptosis and tumor necrosis, and second inhibiting tumor angiogenesis by reducing the expression of pro-angiogenetic factors in tumor tissues and disrupting their pro-angiogenetic activities. Beside these contributions, other factors might be also responsible for the strong tumor cytotoxicity of this nanoparticles-drug system, including the preferential accumulation of MSNs in tumor sites as described in the previous studies,[13,14] the MSNs-mediated endocytosis and the

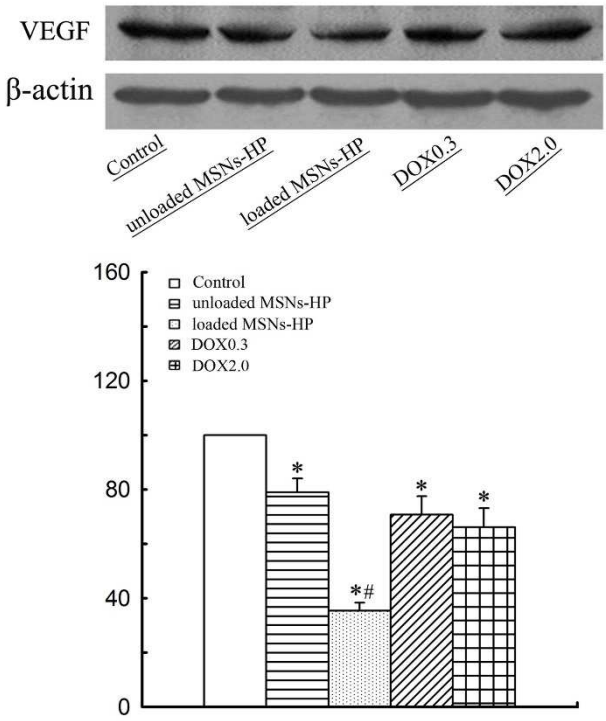

Fig. 8 The expression of VEGF in the tumor tissue of transplanted H22 mice treated with different agents. (* $P < 0.05$ *vs* control group and $^{\#}$ $P < 0.05$ *vs* DOX2.0 group).

sustained intracellular release of the DOX drug as indicated by the in vitro/in vivo release profile in Fig. 3. Recently, a global gene expression analysis technology was used by Shi et al for exploring the underlying pathways and mechanisms of cancer cell death induced by MSN-mediated drug delivery.[32] They found that by virtue of a certain kind of synergetic biological effect between nanoparticles and drug, DOX@MSNs DDS was capable of increasing the intracellular levels of reactive oxygen species and triggering the mitochondria-related autophagic lysosome pathway, thus activating a specific pathway of necrosis different from those by the free drug and the carrier molecules. Since the strong antitumor effect of loaded MSNs-HP also involved the synergetic effect between nanoparticles and drug, the possibility of a unique antitumor mechanism generated by this system could not be ruled out. Further investigation at the molecule level is needed in the future. Herein, it should be noteworthy that the above two types of synergetic effects between MSNs nanoparticles and anticancer drug were observed from different levels. One was from cell level and another was from animal level.

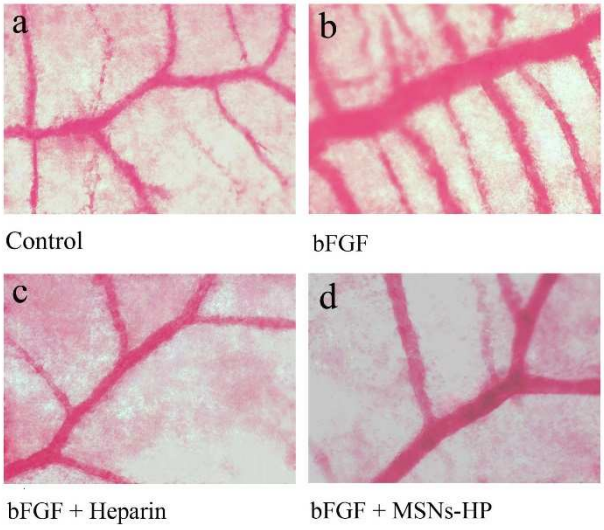

Fig. 9 The effects of different agents on the bFGF-induced tube formation of CAM.

Safety evaluation

As loaded MSNs-HP might induce damage in the organs and tissues of the transplanted mice except the tumor areas, its safeness was examined at the end of experiment. As shown in Table 1, the weight of the mice treated with loaded MSNs-HP was not statistically different from those of the other agents. Furthermore, slightly decreased creatinine/BUN (representative for renal function) and significantly elevated ALT/AST (representative for liver function) were seen in the mice treated with DOX2.0 compared to those of the control mice, whereas the levels of these biomarkers from the other agents were lower than those of the control mice (Table 2). Finally, unmodified white blood cell count and thymus and spleen indexes were observed in all mice except the DOX2.0-treated mice (Table 3). According to these data, it can be seen that in these agents, only DOX2.0 caused unexpected side effects and the others did not show any effects on the normal growth of the transplanted H22 mice, which means loaded MSNs-HP was safer than large doses of the DOX drug, and thus the use of MSNs-HP not only could improve the efficacy of DOX but also reduce its side effect. As for the low toxicity of this system, we speculated that it might be relative to the preferential accumulation of MSNs in tumor sites and its low doses of administration. The details await the further investigations for its biodistribution and clearance profiles in vivo in the future.

Table 2 Blood biochemistry in transplanted H22 mice treated with different agents. (mean ± S. D., n = 10)

Groups	Creatinine (mg dL^{-1})	BUN (mg dL^{-1})	ALT (U L^{-1})	AST (U L^{-1})
Control	65.2 ± 4.6	8.7 ± 0.9	52.8 ± 7.8	872.5 ± 231.5
unloaded MSNs-HP	66.5 ± 7.6	8.8 ± 1.1	43.5 ± 6.2$^{*\#}$	674.4 ± 180.2$^{*\#}$
loaded MSNs-HP	65.1 ± 9.0	8.7 ± 2.7	38.4 ± 5.1$^{*\#}$	558.1 ± 175.1$^{*\#}$
DOX0.3	61.3 ± 7.7	7.3 ± 1.2	39.5 ± 9.5$^{*\#}$	562.0 ± 175.4$^{*\#}$
DOX2.0	60.5 ± 6.9	7.0 ± 1.2	57.3 ± 15.6	1181.2 ± 325.5*

* $P < 0.05$, compared to control group; $^{\#}$ $P < 0.05$, compared to DOX2.0 group.

Table 3 Influence of different agents on immune function of transplanted H22 mice (mean ± S. D., n = 10)

Groups	White blood cell count($\times 10^{9}$ L^{-1})	Thymus index ($\times 10^{-3}$)	Spleen index ($\times 10^{-3}$)
Control	6.1 ± 1.2	2.2 ± 0.4	8.9 ± 0.1
unloaded MSNs-HP	7.6 ± 1.3	2.5 ± 0.1$^{\#}$	8.5 ± 0.2$^{\#}$
loaded MSNs-HP	7.8 ± 1.1	2.2 ± 0.8$^{\#}$	8.5 ± 0.3$^{\#}$
DOX0.3	7.2 ± 0.7	2.0 ± 0.4$^{\#}$	9.6 ± 0.2$^{\#}$
DOX2.0	7.4 ± 1.4	1.0 ± 0.6*	3.9 ± 1.9*

* $P < 0.05$, compared to control group; $^{\#}$ $P < 0.05$, compared to DOX2.0 group.

Conclusions

In this study, the synthesis and characterization of heparinized mesoporous silica nanoparticles MSNs-HP were described firstly. Then, MSNs-HP was found capable of penetrating into cancer cells and delaying the release of anticancer drug DOX in vitro/in vivo. Much interesting, in vivo investigations using animal xenograft models showed that only carrying a few amounts of drug could loaded MSNs-HP achieve the similar antitumor efficacy as that large doses of drug alone. Such a strong tumor cytotoxicity of this nanoparticles-drug system could be correlated to the synergistic effect of these two components in inducing tumor cell apoptosis and tumor necrosis and inhibiting tumor angiogenesis. Furthermore, this system was found safer than large doses of drug. All the above might enable MSNs-HP to be a potentially high-efficiency and

low toxicity carrier for anticancer drug delivery. However, considering the possible anticoagulant side effect, the in vivo evaluation was performed only at the low dose range of these heparinized nanoparticles. To increase the use dosage, we intend to modify the surfaces of MSNs with non-anticoagulant and antiangiogenetic heparin derivatives in the next stage.[33-35]

Acknowledgements

The authors should be grateful to the financial support of the National Natural Science Foundation of China (grant no. 21471046), the Important National Science & Technology Specific Projects (grant no. 2012ZX09301003-001-009) and the State Key Laboratory of Antitoxic Drugs and Toxicology.

Notes and references

[a] *College of Pharmacy, Institute of Chinese Material Medical, Henan University, Kaifeng 475004, PR China. Email: henuwuqiang@henu.edu.cn*

[b] *Department of Pharmacology, Medical College, Henan University of Science and Technology, Luoyang 471003, PR China. Email: ylliruifang@163.com*

[c] *Department of Pharmaceutics, Beijing Institute of Pharmacology and Toxicology, Beijing 100850, PR China.*

Electronic Supplementary Information (ESI) available: [Zeta potential of nanoparticles]. See DOI:10.1039/b000000x/

1 M. M. Kemp and R. J. Linhardt, *WIRES Nanomed. Nanobi.*, 2010, **2**, 77.
2 M. D. Sharath, Z. M. Merchant, Y. S. Kim, K. G. Rice, R. J. Linhardt and J. M. Weiler, *Immunopharmacology*, 1985, **9**, 73.
3 J. M. Weiler, R. E. Edens, R. J. Linhardt and D. P. Kapelanski, *J. Immunol*, 1992, **148**, 3210.
4 G. Liu, M. Hultin, P. Oestergaard and T. Olivecrona, *Biochem. J.*, 1992, **285**, 731.
5 R. Crum, S. Szabo and J. Folkman, *Science*, 1985, **230**, 1375.
6 J. Folkman, R. Langer, R. J. Linhardt, C. Haudenschild and S. Taylor, *Science*, 1983, **221**, 719.
7 K. Park, G. Y. Lee, Y. S. Kim, M. Yu, R. W. Park, I. S. Kim, S. Y. Kim and Y. Byun, *J. Control. Release,* 2006, **114**, 300.
8 C. Passirani, G. Barratt, J. P. Devissaguet and D. Labarre, *Pharm. Res*., 1998, **15**, 1046.
9 M. H. Dufresne and J. C. Leroux, *Pharm. Res*., 2004, **21**, 160.
10 K. Na, K. Park, S.W. Kim and Y. H. Bae, *J. Control. Release*, 2000, **69**, 225.
11 S. Kwon, J. H. Park, H. Chung, I. C. Kwon and S. Y. Jeong, *Langmuir*, 2003, **19**, 10188.
12 H. Meng, M. Xue, T. Xia, Z. Ji, D. Y. Tarn, J. I. Zink and A. E. Nel, *ACS Nano*, 2011, **5**, 4131.
13 V. Mamaeva, J. M. Rosenholm, L. T. Bate-Eya, L. Bergman, E. Peuhu, A. Duchanoy, L. E. Fortelius, S. Landor, D. M. Toivola, M. Linden and C. Sahlgren, *Mol. Ther*., 2011, **19**, 1538.
14 J. Lu, M. Liong, Z. Li, J. I. Zink and F. Tamanoi, *Small*, 2010, **6**, 1794.
15 H. Meng, M. Xue, T. Xia, Z. X. Ji, D. Y. Tarn, J. I. Zink and A. E. Nel, *ACS Nano*, 2011, **5**, 4131.
16 Q. J. He, J. M. Zhang, J. L. Shi, Z. Y. Zhu, L. X. Zhang, W. B. Bu, L. M. Guo and Y. Chen, *Biomaterials*, 2010, **31**, 1085.
17 M. Gary-Bobo, Y. Mir, C. Rouxel, D. Brevet, I. Basile, M. Maynadier, O. Vaillant, O. Mongin, M. Blanchard-Desce, A. Morere, M. Garcia, J.-O. Durand and L. Raehm, *Angewandte. Chemie*, 2011, **123**, 11627.
18 Q. Wu, C. Liu, L. Fan, J. Shi, Z. Liu, R. Li and L. Sun, *Nanotechnology*, 2012, **23**, 485703.
19 H. J. Chung, H. K. Kim, J. J. Yoon and T. G. Park, *Pharm. Res*., 2006, **23**, 1835.
20 L. P. Zhu, J. Xing, Q. X. Wang, L. Kou, C. Li, B. Hu, Z. W. Wu, J. J. Wang and G. X. Xu, *Eur. J. Pharmacol*., 2009, **617**, 23.
21 K. Le, R. Li, S. Xu, X. Wu, H. Huang, Y. Bao, Y. Cai, T. Lan, J. Moss, C. Li, J. Zou, X. Shen and P. Liu, *Arch. Biochem. Biophys*., 2012, **518**(1), 71.
22 R. Li, W. Zheng, R. Pi, J. Gao, H. Zhang, P. Wang, K. Le and P. Liu, *FEBS Lett*., 2007, **581**, 3311.
23 A. Saleem, M. Husheem, P. Harkonen and K. Pihlaja, *J. Ethnopharmacol*., 2002, **81**, 327.
24 H. Chen, L. You and S. Li, *Cancer Lett*., 2004, **211**, 163.
25 Z. Q. Yu, R. M. Schmaltz, T. C. Bozeman, R. Paul, M. J. Rishel, K. S. Tsosie and S. M. Hecht, *J. Am. Chem. Soc.*, 2013, **135**, 2883.
26 T. Sato, M. Hanada, S. Bodrug, S. Irie, N. Iwama, L. H. Boise, C. B. Thompson, E. Golemis, L. Fong and H. G. Wang, *Proc. Natl. Acad. Sci. USA*, 1994, **91**, 9238.
27 M. J. Cross and L. Claesson-Welsh, *Trends Pharmacol. Sci*,, 2001, **22**, 201.
28 N. Tarasenko, S. M. Cutts, D. R. Phillips, A. Inbal, A. Nudelman, G. Kessler-Icekson and A. Rephaeli, *PLoS ONE*, 2012, **7**, e31393.
29 M. M. Kemp, A. Kumar, S. Mousa, E. Dyskin, M. Yalcin, P. Ajayan, R. J. Linhardt and S. A. Mousa, *Nanotechnology*, 2009, **20**, 455104.
30 Y. Matsumura and H. Maeda, *Cancer Res*., 1986, **46**, 6387.
31 H. Maeda, J. Wu, T. Sawa, Y. Matsumura and K. Hori, *J. Control. Release,* 2000, **65**, 271.
32 X. Li, Q. He and J. Shi, *ACS Nano*, 2014, **8**, 1309.
33 L. Lundin, H. Larsson, J. Kreuger, S. Kanda, U. Lindahl, M. Salmivirta and L. Claesson-Welsh, *J. Biol. Chem*., 2000, **275**, 24653.
34 Y. Yoshitomi, H. Nakanishi, Y. Kusano, S. Munesue, K. Oguri, M. Tatematsu, I. Yamashina and M. Okayama, *Cancer Lett*., 2004, **207**, 165.
35 K. Ono, M. Ishihara, K. Ishikawa, Y. Ozeki, H. Deguchi, M. Sato, H. Hashimoto, Y. Saito, H. Yura, A. Kurita and T. Maehara, *Br. J. Cancer*, 2002, **86**, 1803.

Gracphical abstract

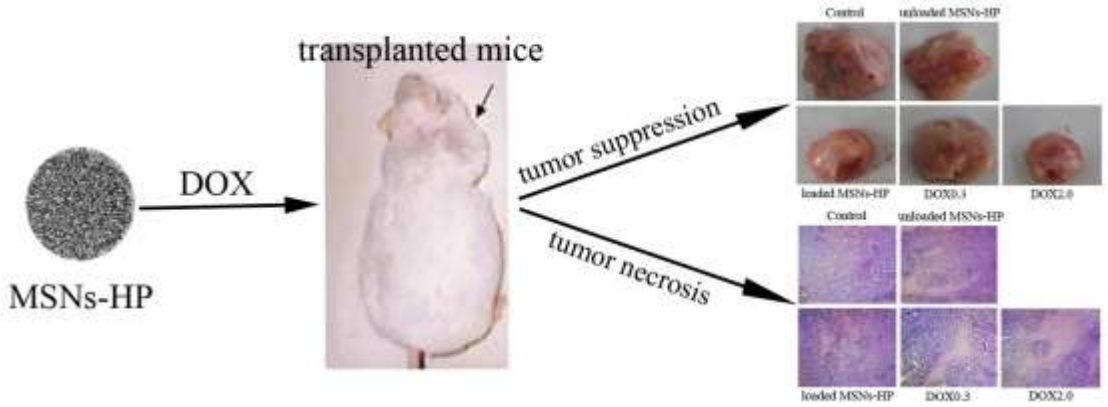

Only carrying a few amounts of drug (DOX0.3) could loaded MSNs-HP achieve the similar antitumor efficacy as that large doses of drug (DOX2.0, 7-fold higher in dosage than DOX0.3).